BNL-107104-2014-JA

Can CO-tolerant Anodes be Economically Viable for PEMFC Applications with Reformates?

J. X. Wang[a], P. He[b], Y. Zhang[a], and S. Ye[b]

[a] Department of Chemistry, Brookhaven National Laboratory, Upton, New York 11973, USA
[b] Ballard Power Systems, Inc., Burnaby, British Columbia V5J 5J8, Canada.

Several years ago, the answer to this question was **negative** based on the criteria for an anode with <0.1 mg cm^{-2} of platinum group metals to perform similarly without and with 50 ppm CO in hydrogen proton exchange membrane fuel cells (PEMFCs). Now, with the amount of CO impurities reduced to 10 ppm in reformates, a <1% performance loss with a 1.5% air-bleed has become a reasonable target. The CO-tolerant catalyst also needs to be dissolution resistant up to 0.93 V, viz., the potential experienced at the anode during startup and shutdown of the fuel cells. We recently demonstrated our ability to simultaneously enhance activity and stability by using single crystalline Ru@Pt core-shell nanocatalysts. Here, we report that the performance target with reformates was met using bilayer-thick Ru@Pt core-shell nanocatalysts with 0.047 mg cm^{-2} Pt and 0.024 mg cm^{-2} Ru loading, supporting a **positive** prognosis for the economically viable use of reformates in PEMFC applications.

Introduction

Recent advances in lowering CO impurity level from 1% to 10 ppm via preferential oxidation (PROX) of CO in hydrogen feeds (1) renewed interest in developing CO-tolerant catalysts for using reformates as an inexpensive fuel for proton exchange membrane fuel cells (PEMFCs). The savings could be considerable since the 2015 price target for hydrogen produced by reforming natural gas is \$2 per kg H_2, viz., ~40% cheaper than pure hydrogen generated by water electrolysis that costs \$3.5 per kg H_2 (2).

To be economically viable, the loss in performance in a reformate-fed PEMFC must be minimal and without a much higher loading of platinum group metals. Currently, the anode Pt loading is targeted at 0.05 mg cm^{-2} for hydrogen PEMFCs (3). Adding CO-tolerance can justify 0.1 mg cm^{-2} for the sum of Pt and Ru. Another challenge comes from the need to prevent the dissolution of Ru at potentials up to 0.93 V. This is because such high potentials can occur at the anode during the startup and shutdown of fuel cells (4), and dissolved Ru can migrate to the cathode, so de-activating Pt catalysts for the oxygen reduction reaction (5, 6).

To maximize Pt utilization and to protect Ru from dissolution, we developed an economically viable method of synthesis to produce single crystalline Ru(core)-Pt(shell) nanoparticles with a tunable Pt shell thickness, denoted as Ru@Pt. By eliminating structural defects, we obtained sharp and ordered Ru-Pt core-shell interfaces that made

possible for us to maximize performance and stability via fine tuning the thickness of Pt shells. The enhanced resistance to Ru dissolution was demonstrated earlier (7). In this study, we focus on meeting the CO-tolerance target with minimal loading of platinum group metals.

Experimental

Briefly, we used the solvent ethanol as the reductant in synthesizing carbon-supported Ru nanoparticles and in coating them with Pt atomic layers (7). We assured a narrow distribution of particle size by first reducing Ru^{3+} to Ru^{2+} in an ethanol solution of $RuCl_3$ via heating the oil bath to 110 ºC, and then assured their complete reduction by adding alkaline solution (about 3 times that of the molar amount of Ru). The filtered and dried Ru/C was annealed in hydrogen at 450 ºC for 1 h to minimize structural defects. A coating of Pt was laid down in an ethanol solution of H_2PtCl_6 with the oil bath's temperature at 80 ºC. If the solution was not colorless after 2 hours, a small amount of an alkaline solution was added to fully reduce the Pt precursor. In both steps, the metal yield was nearly 100% as verified by the catalyst's dry weight being consistent with the amount we calculated from the materials we used. For an average particle size about 3.5 nm, the Pt shell thickness varies from 1 to 2 atomic layers, while the Pt:Ru atomic ratio increased from 0.5 to 1.

Catalyst inks were made with a Nafion:carbon weight ratio of 1:1 using a mixed solvent containing water, isopropanol, and ethanol. The inks were well mixed by shaking and sonicating them before we brushed them on to the gas diffusion layers (Ballard Material Products or Sigracet GDL 25 BC). The metal loading was determined from the dry weight of coated catalysts, with the metal percentages based on the materials used in the synthesis and ink preparation.

Fuel cell performance was tested on membrane electrode assemblies (MEAs) with an active electrode area of 45 cm^2. The cathode catalyst was Pt/C (Pt loading: 0.4 mg cm^{-2}), the membrane was Nafion®211, and the gas diffusion layers were obtained from Ballard Material Products. The CO stripping measurements in MEA were performed by purging the anode with 1% CO balanced with N_2 and then with N_2 alone. The potential sweep rate was 20 mV s^{-1} and the cathode was under H_2 flow.

Results and Discussions

Screening Test using GDE Strips in 1 M $HClO_4$ Solutions

To identify the optimal Ru:Pt atomic ratio and the ratio of total metal weight to carbon support, we conducted screening tests using gas diffusion electrodes (GDEs) in solution electrochemical cells with a Pt counter electrode and an Ag/AgCl reference electrode. The rate of gas flow was kept constant and a three-way valve was used to switch between hydrogen without and with 270 ppm CO. Figure 1 a-c present the results for six GDE samples; Table I summarizes their components and the performance parameters. We used a consistent color code in the three plots and in the Table.

TABLE I. Sample components and results from GDE strips tested in 1 M $HClO_4$ solution.

Sample label	1	2	3	4	5	6
Ru:Pt atomic ratio	0	0.75	1	1	1	2
Total metal weight %	45	52	47	47	37	29
Pt (μg cm^{-2})	67	56	55	23	24	20
Ru (μg cm^{-2})	0	22	28	12	12	21
C (μg cm^{-2})	82	72	94	39	62	103
Estimated A_{Pt} / $A_{Electrode}$	37	49	55	23	24	40
CTR (Ω cm^2) with H_2 and 270 ppm CO	0.78	0.56	0.28	0.35	0.52	1.0
% loss in current with 270 ppm CO	41	39	36	36	49	46
% loss in current after switch back to H_2	16	4	1	2	8	11

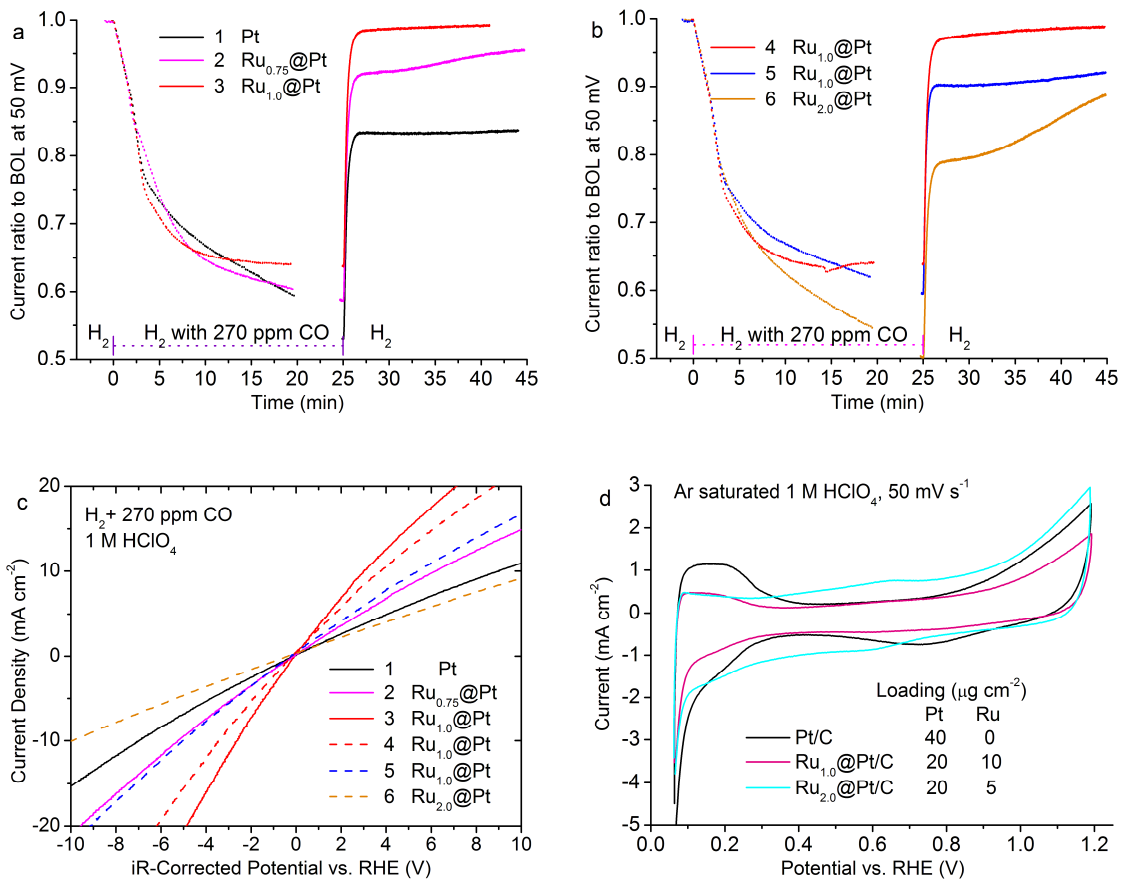

Figure 1. Performance for hydrogen oxidation reaction measured on six GDE samples in a 1 M $HClO_4$ solution at 23 °C. (a,b) The change of currents at 50 mV relative to that at the beginning of the life (BOL) in H_2 as a function of time with the gas inlet switched at 0 and 25 min. (c) iR-corrected polarization curves measured after 20 min with 270 ppm CO in H_2. (d) Typical voltammetry curves for Pt/C, bilayer Ru@Pt/C, and monolayer Ru_2@Pt/C catalysts measured in Ar-saturated 1 M $HClO_4$ solution.

We labeled the samples in sequence with increasing Ru:Pt atomic ratio (second row), and then with decreasing total metal weight percentage (third row). Samples #3 and #4 were made with the same catalysts, differing only in loading. One is in the relatively high loading group of samples #1-3, and another in the lower loading group of samples #4-6.

The loadings were determined from measured weights and thus slightly differ within the group. Table I gives the ratios of Pt surface area (A_{Pt}) to electrode surface area ($A_{electrode}$) that were estimated based on a Pt specific surface area of 1.0 cm^2 μg^{-1} for the 1:1 Ru:Pt atomic ratio bilayer catalyst determined using the CO striping charge, and that of 0.56 cm^2 μg^{-1} for the Pt/C determined by the hydrogen adsorption charge.

We show in Figures 1a and 1b the changes in the hydrogen oxidation reaction (HOR) currents at 50 mV upon switching to CO-containing hydrogen at 0 min and switching back to pure hydrogen at 25 min. There is a 5 minute gap between the two parts of curves because we measured polarization curves and high frequency resistances during that time; they yielded the iR-corrected polarization curves shown in Figure 1c. From the slopes obtained by linear fitting near 0 V, we determined the values of the charge transfer resistances (CTRs) that we list in Table I to quantify the activity on an absolute scale. We note that the activity is proportional to 1 / CTR, i.e., a lower CTR represents a higher activity. In relative terms, the losses in performance due to CO adsorption are expressed in percentages for the currents at 50 mV measured 20 min after introducing CO-containing hydrogen, and then after 20 min recovery in pure hydrogen, both with respect to that at the beginning of the life (BOL) in hydrogen (the last two rows in Table I).

The lowest CTR and percentage losses indicate the best performance; they were obtained with the catalyst having 1:1 Ru:Pt ratio and 47% metal weight (#3 and #4). Without the Ru core (#1), the HOR current had not stabilized after 20 min in the presence of CO, and then recovered poorly after switching back to pure hydrogen (Figure 1a). The sample made with 3:4 Ru:Pt atomic ratio (#2) exhibited a behavior in between those of #1 and #3, indicating that going beyond the thickness of a bilayer shell made the surface property too close to that of pure Pt nanoparticles (#1). For the low loading group (Figure 1b), increasing the metal weight percentage from 37% (#5) as in our previous studies to 47% (#4) in this work had a positive effect, probably due to a more compact catalyst layer. The monolayer catalyst with Ru:Pt atomic ratio of 2:1 performed poorly, consistent with the trend we found previously (7).

The change of surface properties with the thickness of Pt shell can be seen in voltammetry curves in Figure 1d. While the hydrogen adsorption current is hard to see on the monolayer Ru_2@Pt/C (light blue), the curve for the bilayer Ru@Pt/C (pink) exhibits features analogous to that of Pt/C, i.e., having a clear double layer region between hydrogen adsorption at low potentials and OH/O adsorption at high potentials. Since the Pt specific surface area for the bilayer Ru@Pt/C is approximately twice that of Pt/C (1.0 versus 0.56 cm^2 μg^{-1}), while the Pt loading is half (20 versus 40 μg cm^{-2}), the two electrodes have about the same Pt surface area. Thus, the lower H and OH/O adsorption currents on the bilayer Ru@Pt/C support that the Pt surface becomes less reactive by interacting with a Ru core. Fortunately, the HOR activity is not affected by weakened hydrogen adsorption, while dissolution resistance is enhanced by weakened O/OH adsorption. In contrast, the high oxidative current at high potentials on the monolayer Ru_2@Pt/C suggests that a Pt monolayer cannot prevent Ru dissolution. This is an additional reason for why the bilayer Ru@Pt/C is the most promising HOR catalysts for PEMFCs. For conventional PtRu/C, Ru even is present in the top surface layer, and thus, dissolution of Ru is a serious problem.

MEA Test with Reformates

We prepared an anode GDE with bilayer Ru@Pt/C at 47% metal weight percentage and tested its performance in PEMFC with a reformate comprising 72% H_2, 20% CO_2, 8% N_2, and 10 ppm CO with 1.5% air bleed and compared it to that with pure hydrogen using Ballard Power Systems' standard protocols. Figure 2 shows that the two polarization curves differ only slightly, and their difference can be fully described by a constant factor in currents, as is evidenced by a curve generated by dividing the currents of the reformate polarization curve (red pluses) by 0.8 (red crosses) that matches the hydrogen polarization curve (blue circles) very well. This fact favors the absence of losing active surface sites due to CO adsorption because otherwise the loss would have become bigger at higher currents, as usually seen. Combining this nearly perfect match over the entire curve with the dilution correcting factor not exceeding 1/0.72 for the 72% H_2 in the reformate, we concluded that the anode performance had no loss due to CO, and thus, met the target of a <1% CO-induced performance loss using a reformate containing 10 ppm CO with 1.5% air bleed. This result is significant because the loading of 0.047 mg cm^{-2} Pt and 0.024 mg cm^{-2} Ru are respectively 50% and 75% lower than the loading needed using conventional PtRu/C catalysts (i.e., 0.1 mg cm^{-2} Pt and 0.1 mg cm^{-2} Ru); Furthermore, the Pt loading is no more than the target for using conventional Pt/C with pure hydrogen.

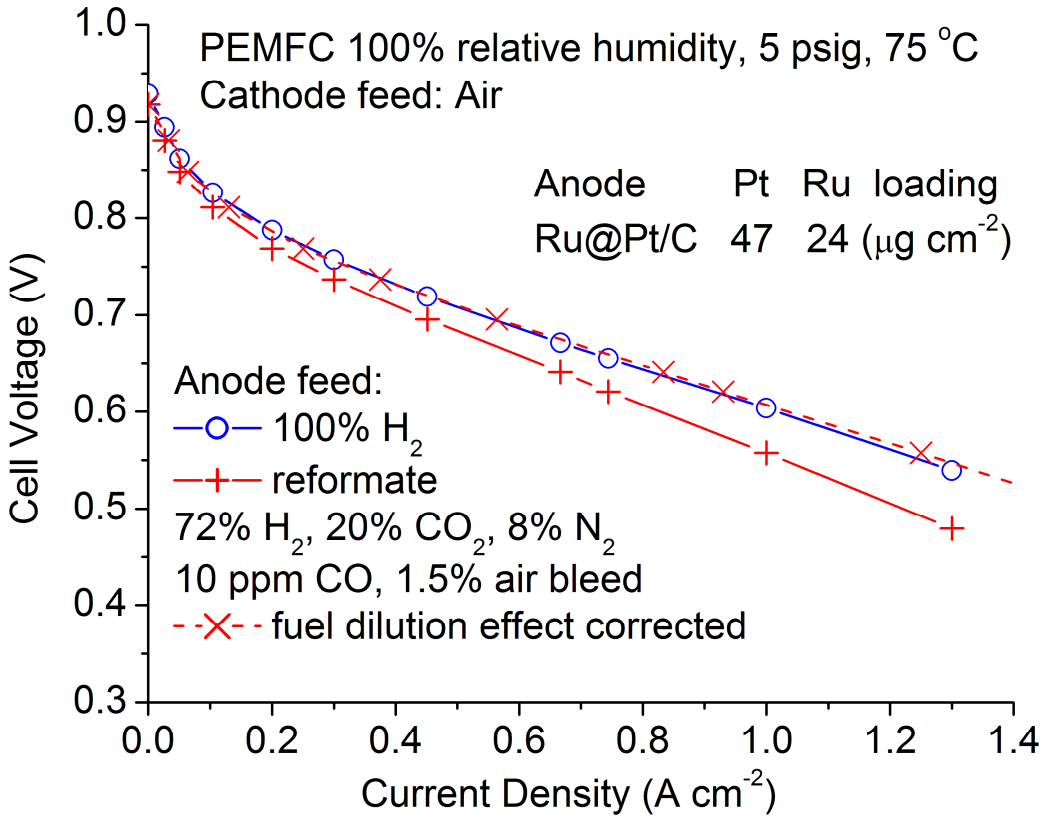

Figure 2. PEMFC polarization curves obtained using an anode comprising bilayer Ru@Pt/C catalysts with pure hydrogen (blue circles) and reformate (red pluses) as the fuel. The curve with red crosses is generated by a correcting factor of 1/0.8 to account for the effects of diluting the fuel.

To characterize the catalysts, we carried out CO stripping measurements in MEA after saturating CO adsorption on the catalysts' with 1% CO in N_2. The surface area ratio A_{Pt} / $A_{electrode}$ was estimated from the measured CO stripping charge (solid blue line in Figure 3) using the commonly assumed value of 0.42 mF cm^{-2}, i.e., twice of the 0.21 mF cm^{-2} hydrogen adsorption charge (8). The value of 48 with a loading of 47 μg cm^{-2} yields a Pt specific area of 48 / 47 = 1 cm^2 μg^{-1} or 100 m^2 g^{-1} for the bilayer Ru@Pt/C catalyst.

Figure 3 also shows that the potential of CO-stripping peak for the bilayer Ru@Pt/C is lower than that for Pt/C and higher than that for a conventional PtRu/C. Because the atomic mass ratio for Ru:Pt is 101/195 = 0.52, the alloy PtRu/C with equal weights of Pt and Ru corresponds to roughly a Ru:Pt atomic ratio of 2. Thus, the Ru contents in the alloy PtRu/C is higher than the 1:1 atomic ratio, bilayer Ru@Pt/C. Besides, having both Ru and Pt at the surface is known to down shift the CO stripping peak potential (9). The effect supports a bifunctional mechanism, wherein Ru sites induce O/OH adsorption at low potentials to facilitate oxidative removal of adsorbed CO molecules at nearby Pt sites. While this mechanism is important for oxidation of methanol and formic acid (10, 11), it is not necessarily so for the HOR with reformates because CO stripping anyway occurs at potential far higher than the anode's operating potential of < 0.1 V for hydrogen PEMFCs. Therefore, we chose to measure the response of the HOR current to the presence of CO at 0.05 V in our screening tests (Table I and Figure 1).

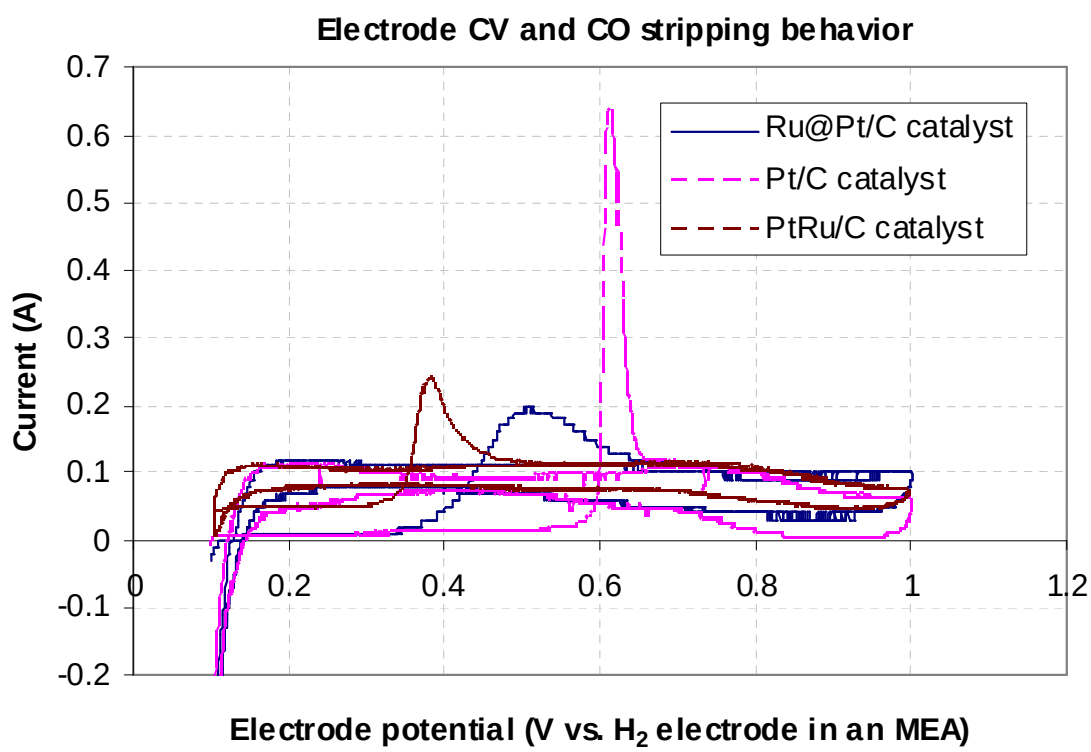

Figure 3. Anode's CO stripping behavior of the bilayer Ru@Pt/C (solid blue line) in comparison with those of conventional Pt/C (pink dashed line) and PtRu/C (brown dashed line) catalysts. The metal loading for the bilayer Ru@Pt/C electrode is 47 μg cm^{-2} Pt and 24 μg cm^{-2} Ru.

Conclusions

A CO-tolerant anode was made using the best performing bilayer Ru@Pt/C catalysts selected by screening test in 1 M $HClO_4$ solutions. With only 47 μg cm^{-2} Pt and 24 μg cm^{-2} Ru metal loadings, the loss in currents with a reformate comprising 72% H_2, 20% CO_2, 8% N_2, and 10 ppm CO with 1.5% air bleed was found only 20% over entire voltage region, that can be fully accounted for by the effect of fuel dilution, with no loss in active sites due to CO adsorption.

This unprecedented performance is achieved by having an atomically sharp, ordered core-shell interface. For operating with reformate in PEMFCs, bilayer is the optimal thickness of Pt shell – providing just right amount electronic influence from a Ru core in optimizing Pt's surface properties, and, at the same, encapsulating Ru with a complete Pt shell to enhance Ru dissolution resistance.

Acknowledgments

Part of this material is based upon work supported by the U.S. Department of Energy Office of Science, Office of Basic Energy Sciences under Award Number DE-AC02-98CH10886.

References

1. K. Liu, A. Wang, T. Zhang, *ACS Catalysis* **2012**, *2*, 1165-1178.
2. Satyapal, S. Fuel Cell Technologies Update, p. 17 in Hydrogen and Fuel Cell Technical Advisory Committee Meeting, Washington, DC (2013). http://www.hydrogen.energy.gov/pdfs/htac_apr13_1_satyapal.pdf.
3. K. C. Neyerlin, W. B. Gu, J. Jorne and H. A. Gasteiger, *Journal of the Electrochemical Society*, **154**, B631 (2007).
4. P. He, T. T. H. Cheng, R. Bashyam, Y. A. P. and K. S., *ECS Trans.*, **33**(1), 1273 (2010).
5. T. T. H. Cheng, N. Y. Jia and P. He, *Journal of the Electrochemical Society*, **157**, B714 (2010).
6. E. Antolini, Journal of Solid State Electrochemistry, **15**, 455 (2011).
7. Y. C. Hsieh, Y. Zhang, D. Su, V. Volkov, R. Si, L. J. Wu, Y. M. Zhu, W. An, P. Liu, P. He, S. Y. Ye, R. R. Adzic and J. X. Wang, *Nature Communications*, **4,** 2466 (2013).
8. M. Bernechea, S. Garcia-Rodriguez, P. Terreros, E. de Jesus, J. L. G. Fierro and S. Rojas, *Journal of Physical Chemistry C*, **115**, 1287 (2011).
9. H. A. Gasteiger, N. Markovic, P. N. Ross and E. J. Cairns, *Journal of Physical Chemistry*, **98**, 617 (1994).
10. H. A. Gasteiger, N. Markovic, P. N. Ross and E. J. Cairns, *Electrochimica Acta*, **39**, 1825 (1994).
11. N. Muthuswamy, J. L. G. de la Fuente, D. T. Tran, J. Walmsley, M. Tsypkin, S. Raaen, S. Sunde, M. Ronning and D. Chen, *International Journal of Hydrogen Energy*, **38**, 16631 (2013).